Interface enhancement with textured surfaces in thin-film flows

Karthik Vigneshwaran MUTHUKUMAR*, Cihan ATES*,
Rainer KOCH, Hans-Jörg BAUER
Institute of Thermal Turbomachinery
Karlsruhe Institute of Technology
Karlsruhe, Germany
*karthik.muthukumar@kit.edu, *cihan.ates@kit.edu

Andrea DÜLL, Fabio ÖHL,
Thomas HÄBER, Olaf DEUTSCHMANN,
Institute for Chemical Technology and Polymer Chemistry,
Karlsruhe Institute of Technology
Karlsruhe, Germany

***Abstract*—The interfacial area between the fluid and gas phases plays a significant role in the diffusion and mass transfer-controlled processes. For reactive transport, as in the CO_2 absorption in thin-film flows, the time scale of the reaction can be much faster than the time scale of the mass transfer. We, therefore, moot that the absorption rates per volume reactor can be increased if the surface renewal at the interface is enhanced via textured surfaces over which the liquid film flows. Realization of this uncharted potential, however, requires a precise understanding of the complex dynamics between the transient film thicknesses, velocity distributions, and modified surfaces. Hence, we need an accurate and sharp representation of the very thin gas-liquid interface and the ability to capture discontinuities, local penetrations, and the mixing of phases at high temporal and spatial resolutions. In this work, to the best of our knowledge, we investigated for the first time how different surface textures influence the film hydrodynamics and how it is reflected onto the interfacial area statistics at steady conditions using Smoothed Particle Hydrodynamics (SPH). In particular, the effect of structured surfaces on the film hydrodynamics is analyzed statistically for two different texture geometries at two different number densities. In addition, the surface wettability effects are investigated parametrically at three different contact angles. We also analyzed whether texturing help to redistribute the liquid phase to eliminate partial wetting observed in cases of smooth surfaces. Results show that (i) variations in film thickness are strongly influenced by both the presence and number density of textures and (ii) textures can increase the interfacial area by at least six times for the tested cases while alleviating the partial wetting problem. The numerical observations are further confirmed by experimental tests, which also show that with the right blend of geometry, orientation, and density of textures, we can potentially enhance the interfacial area for practical problems such as CO_2 absorption.**

I. Introduction

The utilization of gas-liquid contact reactors is a popular strategy in the chemical industry for dealing with interfacial transport problems, such as passive cooling systems, gas cleaning units, and chemical absorbers. The contact reactors include fixed-bed and bubble columns, membrane reactors, and falling-film reactors. The latter refers to a gas-liquid contactor, where the liquid film flows down a wall or pipe under the influence of gravity, and the gas is conducted counter-currently. Falling-film reactors are mainly characterized by very good heat and mass transfer characteristics and are used in chemical processes (e.g., hydrogenation, sulfonation, chlorination, CO_2 absorption).

In falling-film absorbers, gas molecules are continuously transported from the gas to the liquid phase. The gas molecules exhibit characteristic concentration profiles depending on the physical and chemical properties of the gas and liquid phase, the operating conditions and the reactor configuration. In the case of CO_2 absorption, the competition between the mass transfer rate at the surface and the reaction rate in the liquid film creates large CO_2 concentration gradients within the liquid film since the characteristic reaction time is typically smaller than the characteristic diffusion time within the film surrounding the liquid phase. This influence of chemical reaction on absorption dynamics is traditionally characterized by an *enhancement factor (E)* that depends on a parameter called *Hatta number (Ha)*, which describes the ratio between the diffusion and the reaction time scale. When $Ha >> 1$, as in CO_2 chemical absorption, all reactions occur within the film, and the yield is dictated by the effective interfacial area achieved per unit volume. In practice, it is possible to enhance the absorption process by a factor of 20 (on average) for the common CO_2 absorbents if the interface dynamics are properly tuned [1], [2]. Therefore, there lies a great opportunity to improve the reactor performance via engineering the gas-liquid interface, which in turn will smoothen the transition of novel technologies such as CO_2 capture in practice. The realization of this potential, however, requires a thorough understanding of the complex interface dynamics, including the transient film thicknesses, velocity distributions, and the simultaneous mass transfer process taking place in a very thin concentration boundary layer ($<100\,\mu m$ [3]).

The use of mathematical modeling to understand the coupled mass transfer and flow dynamics at gas-liquid interfaces has been extensively researched for many years. One popular method for modeling gas-liquid contact reactors involves using enhancement factor E models, which date back to the early 1900s. Over time, several models have been developed for different gas-liquid mass transfer problems. The expression of E's dependence on the dimensionless group Ha varies depending

on the approach used to approximate mass transfer dynamics, such as the film, penetration, and surface renewal theories [4]. However, these simplified models fail to reproduce experimental measurements, even for temporally and spatially averaged CO_2 mass transfer rates, for various operational conditions [5]. Recently, there has been a trend towards approximating film dynamics analytically by combining diffusion and reaction source terms through linearization or empirical correlations [6], which also cannot fully capture the dynamic behavior of the interface [7].

A more comprehensive method for analyzing mass transfer across the interface involves using computational fluid dynamics (CFD), which can offer insights into the coupled fluid dynamics and reactive transport across the film that are not easily obtainable from experiments. However, progress in simultaneously solving the two-phase Navier-Stokes and mass transfer equations has been limited compared to stand-alone free surface flow problems [8], despite being an active research field. The main difficulties in reactive transport modeling arise from the significant jumps in density, species concentration, and viscosity across the undulating liquid-gas interface, which necessitates (i) an accurate and sharp depiction of the gas-liquid interface, (ii) the ability to capture discontinuities, local penetrations, and phase mixing, (iii) high temporal and spatial resolutions, (iv) ease of incorporating chemical kinetics, (v) the ability to track reaction fronts on top of the interface tracking, and (vi) computational efficiency on parallel architectures.

Most of the available studies investigating the interface motion in multiphase flows are limited either to momentum transfer [9], [10] and/or mass transfer across the interface without chemical reaction [11], [12]. From a chronological point of view, the first continuous concentration profiles were implemented on both sides of the interface [13]. In the following years, mass transfer calculations were extended to include thermodynamic equilibrium for species transport, which introduced the jump concentration profiles into the computational domain within the VoF method [14]. In the case of the level set method, concentration discontinuity was solved with a special transformation function coupled to the one-fluid formulation for a single droplet [15]. This transformation made the modified variables continuous at the interface by introducing more unknowns in an attempt to satisfy mass flux continuity, which complicated the implementation of the method. More advanced representations of the concentration jumps have been implemented in the following years deploying sophisticated algorithms as in [16].

Despite these improvements, the biggest challenge in the field of interfacial mass transfer still remains. In a typical gas-liquid system, the thickness of the concentration boundary layer is much smaller than the hydrodynamic boundary layer, for which the ratio reciprocally scales with the square root of the Schmidt (Sc) number [17]. Considering the range of the Sc number in these applications (100-1000), additional computational techniques are needed to resolve the concentration boundary layer. For instance, Darmana et al. [18] used the immersed boundary method to track the interfacial mass transfer and had to implement a mesh three times finer than the hydrodynamic mesh for the convergence of species even for Sc = 1. While a non-reactive boundary layer with a high Sc is already challenging, the complexity of the problem drastically increases for reactive transport as the concentration profile is further steepened by the reactions. This challenge has been addressed in a couple of studies to some extent. In one case [19], the problem was a 2D stationary bubble solved on fixed mesh, while in the other [20] level set method was used for modeling the reactive transport for a 2D droplet. In a more recent work [21], reactive transport around a deformable gas bubble rising in a liquid phase was investigated. An important highlight of the study is the fact that they carried out the hydrodynamic computations on a 200 × 600 grid, whereas the mass transport calculation was performed with a grid resolution of 2000 × 6000. It should also be reminded that momentum and mass transfer equations are solved sequentially, and the solutions obtained at different grid resolutions must be remapped between the solvers, which creates another difficulty. The other alternative is the utilization of sub-grid scale models, which have been used for deformable gas bubbles in liquid [16]. However, their utilization in reactive transport is not straightforward [22] and, at best, is limited to the application range of the deployed model. As also can be seen from the examples, the main application of grid-based solutions is related to hydrodynamically less complicated problems, such as single droplets [23] or rising bubbles [16], [24], compared to the dynamic nature of the wavy interface observed in gas-liquid thin film reactors. Another issue is related to the interface representation within the computational cells. For instance, in the VoF approach, the interface is calculated from the volume fraction function, which tracks the volume of fluids in computational cells rather than the interface itself. Then, in mass transfer calculations, the gradient of volume fraction is utilized to calculate the effective mass transfer area for the source term, which is further coupled with a sub-grid mass transfer model such as Higbie to evaluate mass transfer rates [3], [25]–[27]. Moreover, the utilization of the volume fractions for calculating the effective physical properties leads to incorrect representations of the true heterogeneous nature observed at the interface [28].

Lagrangian methods offer an alternative to alleviate these issues, for which Smoothed Particle Hydrodynamics (SPH) is a strong candidate. The advantage of the SPH is its ability to handle the interface even at high density-viscosity ratios in a natural and straightforward way. In particular, as the continuum is represented by the Lagrangian fluid elements, the position of the interface is immediately defined by the particles' positions. Hence, no reconstruction or tracking algorithm is required. The same is true for the physical properties, as they are stored for each fluid type within the Lagrangian particles. The objective of the current work is to assess the potential of surface texturing in increasing the effective surface

area between the liquid (solvent) phase and the gas phase. To achieve this goal, we performed simulations of falling films on surfaces with two different textures and two different number densities under three different wettability conditions. The objective is to investigate whether texturing can help redistribute the liquid phase and eliminate the partial wetting observed on smooth surfaces at low Reynolds (Re) numbers.

II. Fundamentals

A. SPH - Schemes

The Lagrangian Smoothed Particle Hydrodynamics (SPH) is used to solve the continuity and Navier-Stokes equations assuming weakly-compressible flow to simulate the multiphase flow. Therefore, the Lagrangian form of the continuity and momentum equation is required to derive the SPH schemes for calculating density ρ, velocity $\vec{v}$, volume forces f, shear stresses τ and static pressure p as a function of space and time t:

$$\frac{D\rho}{Dt} = -\rho\left(\vec{\nabla}\cdot\vec{v}\right), \tag{1}$$

$$\rho\frac{D\vec{v}}{Dt} = -\vec{\nabla}p + \vec{\nabla}\cdot\tau + \rho\vec{f}. \tag{2}$$

The physical domain is spatially discretized into particles. The mass of the domain is distributed evenly between the particles and is set constant. Hence, mass is conserved inherently. The density field is computed as per Espanol et al. [29]. The pressure gradient is discretized symmetrically to conserve linear momentum. Viscous forces are calculated by the formulation of Hu and Adam [30], and surface tension by the Continuum Surface Force model [31]. Pressure is determined using the Tait equation following the weakly compressible approach, with additional background pressure to avoid tensile instability [32]. In every simulation, particles are flagged by individual ID numbers, which allow tracking each particle inside the computational domain at each time step.

III. Computational Setup

One of the motives for introducing textures to the reactor wall is to decrease the contact angle, thereby increasing wettability and alleviating partial wetting completely. Because texturing affects the surface roughness and with the right combination of texture properties, one can decrease the contact angle between liquid and solid. Hence the work interests in studying the effect of contact angles on film hydrodynamics. Therefore, three test cases with increasing contact angles, namely 20°, 30°, and 40°, are studied. These initial studies are done in 2D to understand the basic effects of texturing extensively by running multiple test trials with different spatial and temporal resolutions at cheaper computational costs.

As for geometry, a computational domain of 0.1×0.005 m is constructed and discretized spatially with particles of size $50\,\mu$m. The liquid and superficial gas velocities are 0.1 ($Re = 55.55$) and 0.75 m/s flowing in a co-current direction in the direction of gravity. The simulation is initialized with pre-wetted walls with a film thickness of $500\,\mu$m based on Nu film thickness, which enables us to have a good initial estimate to reach steady-state flow conditions faster. For textures, two different geometries with two frequencies are chosen. Hence, for each contact angle, we have four test cases with texture and one test case with a flat reactor wall (Figure 1) :

1) T1 – Base case with no textured walls
2) T2 – Box-shaped textures of length $300\,\mu$m and breadth $100\,\mu$m separated by a distance $x = 300\,\mu$m
3) T3 – Box-shaped textures of length $300\,\mu$m and breadth $100\,\mu$m separated by a distance $x = 600\,\mu$m
4) T4 – Semi-circle-shaped textures of length $300\,\mu$m and breadth $100\,\mu$m separated by a distance $x = 300\,\mu$m
5) T5 – Semi-circle-shaped textures of length $300\,\mu$m and breadth $100\,\mu$m separated by a distance $x = 600\,\mu$m

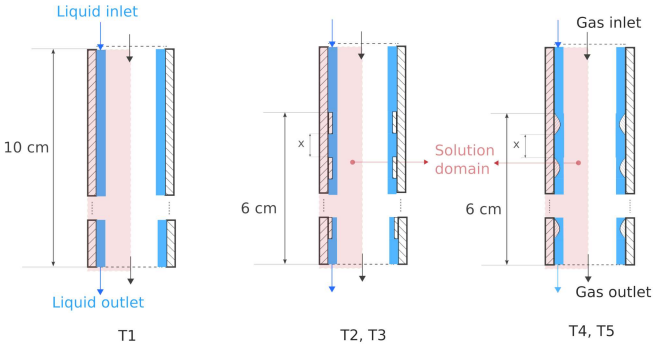

Fig. 1. Reactor geometry with different textures

All test cases were run till a physical time of at least 7 seconds with a temporal resolution of 1.1MHz ($\Delta t \sim 0.9$ ns). The film statistics were calculated between $4 - 7s$, and parametric quantities, such as positions, velocity components, pressure, density, fluid type, and unique particle IDs, were exported at 250 Hz. This voluminous data is then post-processed to extract the local film thicknesses and fluid interfacial length at regular frequencies. Data is read by placing "virtual probes" along the reactor wall at 0.02 m, 0.04 m, and 0.07 m downstream from the inlet.

IV. Experimental Setup

Parallel to the numerical investigations, we performed an experimental campaign to create a benchmark dataset for liquid film thickness and liquid distribution measurements. The measurements are done in two steps: (i) chromatic confocal distance measurement (Precitec, CHRocodile 2S 3 mm-sensor) for point-wise film thickness measurements that are used to assess the impact of film waviness and (ii) an in-house developed light absorption method to quantify the liquid distribution over the plate and film thickness distribution over the surface. All plates were designed in Autodesk Inventor Professional 2023 and fabricated in-house from Plexiglas. All structures were

created both in-flow and orthogonal to the flow directions with changing sizes and number densities.

Figure 2(a) shows the experimental setup for chromatic confocal distance measurement. The dye solution reservoir (1) is connected to pump (2) via a fabric hose. The liquid reservoir (3) is also connected to the pump via a fabric hose. The vent valve (4) is connected to the liquid reservoir (3) via a hose. The outlet hose (5) hangs in a collecting container with a capacity of 20 liters. The measuring head (6) has a measuring range of 3 mm. In this case, the light spot of the measuring head is focused on the lower part of the falling film. In the experiments, the sensor was focused on different positions on the falling film. The measuring head is connected to the sensor (7) via a fiber optic cable. Figure 2(b) depicts the experimental setup for the light absorption method. Numbers 1 to 5 are identical to Figure 2(a). Number 6 in this setup corresponds to a Nikon DSLR camera, and number 7 corresponds to an LED panel used as a light source. The experiments using the light absorption method are carried out with the room lighting turned off to prevent the recordings from being distorted by light not coming from the LED panel. In addition, the laboratory windows are covered with aluminum foil to prevent measurements from being distorted by daylight. The collected images are then post-processed via a calibration curve to convert pixels to film thicknesses in the Matlab environment.

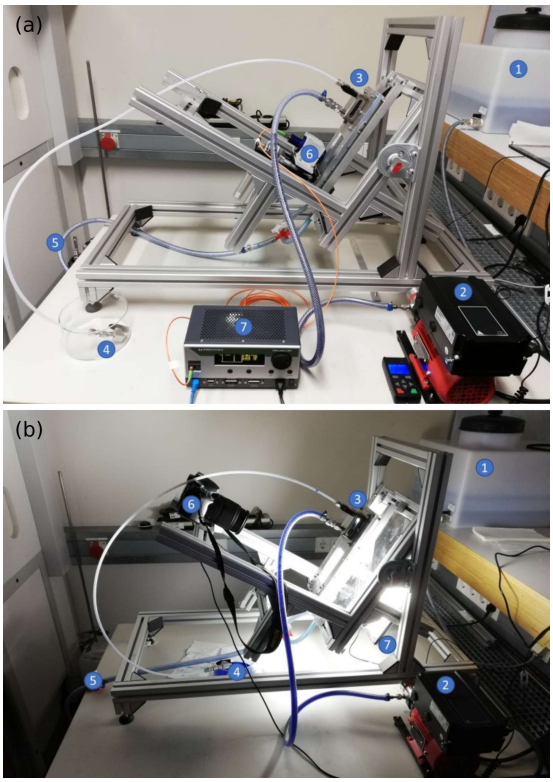

Fig. 2. Experimental setup for chromatic confocal distance measurement and surface film thickness measurement with light absorption.

V. Results and Discussions

A. Parametric study on wettability effects

In the initial parametric study, we examined how wettability affects the statistics of film thickness. However, it is important to note the film's Reynolds number (Re) before discussing the results. Since Re significantly affects the film's flow, it is essential to determine the film's Re to anticipate its behavior. For this numerical setup, the value of $Re = 55.55$ is calculated from the Nusselt film thickness value. With such a low Re, partial wetting ([33], [34]) can be expected, as evidenced by the film thickness vs. time plot (Figure 3). In Fig. 3, there are two plots shown. The left column shows the film thickness vs. time plot for each contact angle with different textures between $4 - 7s$. The right column shows a Fast-Fourier transform on the film thickness values for all cases and displays a frequency vs. amplitude graph. The results were taken at a distance of 7cm from the inlet downstream of the reactor.

The plot of film thickness reveals two important findings. First, partial wetting becomes more severe in the absence of textures with increasing contact angles. Second, the introduction of textures completely eliminates the issue of partial wetting, regardless of the textures and contact angles used. The graph also demonstrates that, for high-density textures ($T2, T4$), the film thickness values vary over a wider range than for low-density textures ($T3, T5$). This indicates that the frequency of textures significantly impacts the film dynamics, with uniform and less spread film thickness for low-density textures.

The Power Spectrum Density (PSD) plot in the right column confirms the previous findings. The X and Y-axes show the frequency and amplitude of the waves, respectively. The PSD analysis indicates that texture frequency can significantly alter the amplitude of the wave components. In particular, low contact angles with high texture density ($T2, T4$) can yield a higher interfacial area due to the presence of high amplitude waves in all frequency ranges. However, for textures $T2$ and $T4$, the waves are more uniformly distributed throughout the frequency spectrum. Moreover, regarding the geometry, the waves tend to be smoother for rounded textures. The observed inconsistencies may be due to the sharp edges acting as obstacles, leading to mild liquid accumulation at the corners. Currently, we are modeling flow over textured surfaces for longer reactor configurations to gain better insights into the relative effects in the developed regime.

B. Texture Effects on Interfacial Area

In this section, we examine the impact of textures and their properties on the gas-liquid interfacial length and the probability distribution of film thickness (Figure 4). We focus solely on the interfacial length and measure it from 0.04m downstream of the reactor, where the structures begin. Herein, the interfacial length refers to the total length of the gas-liquid interface in the 2D simulations at a given time t.

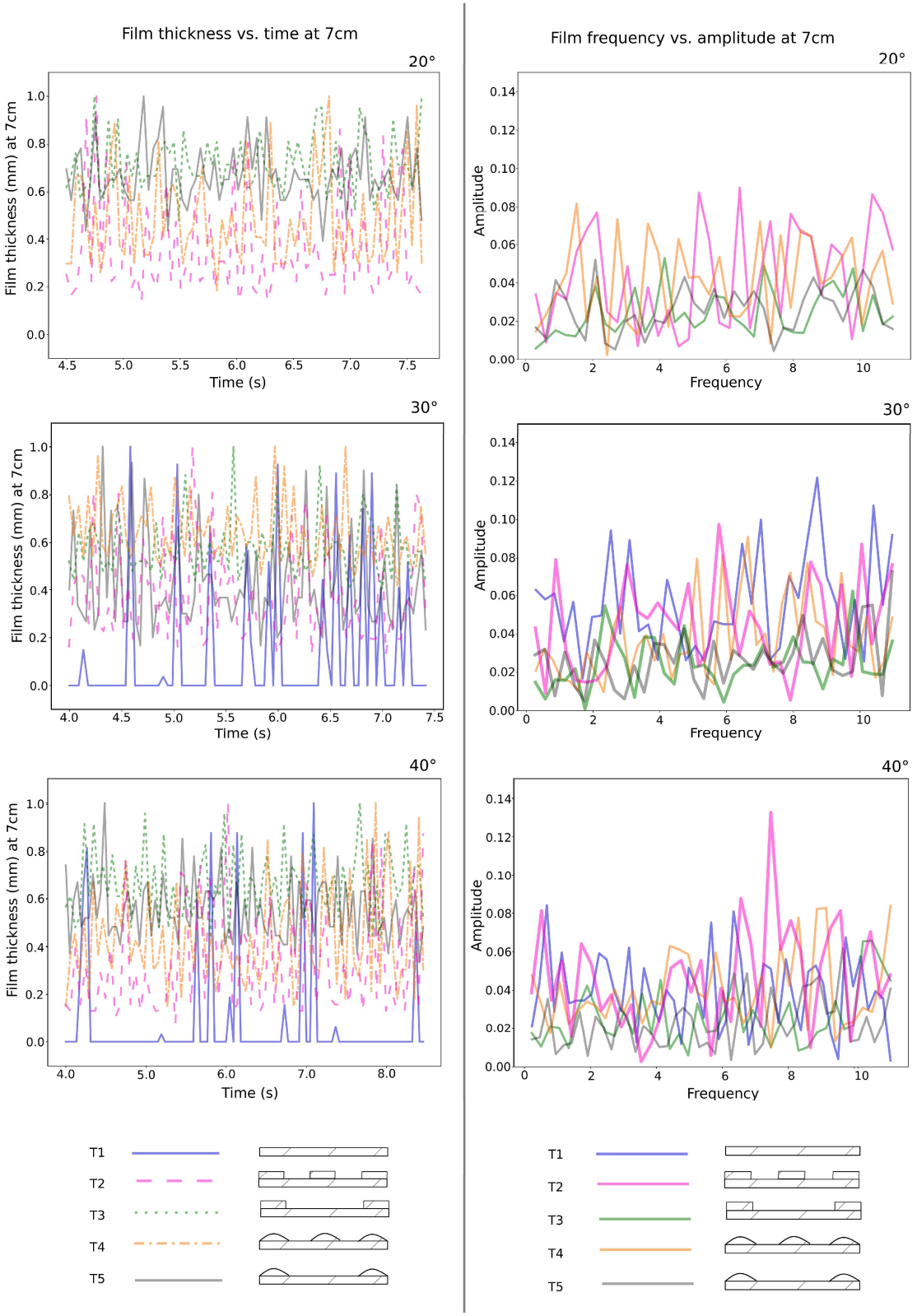

Fig. 3. Effect of textures on wettability

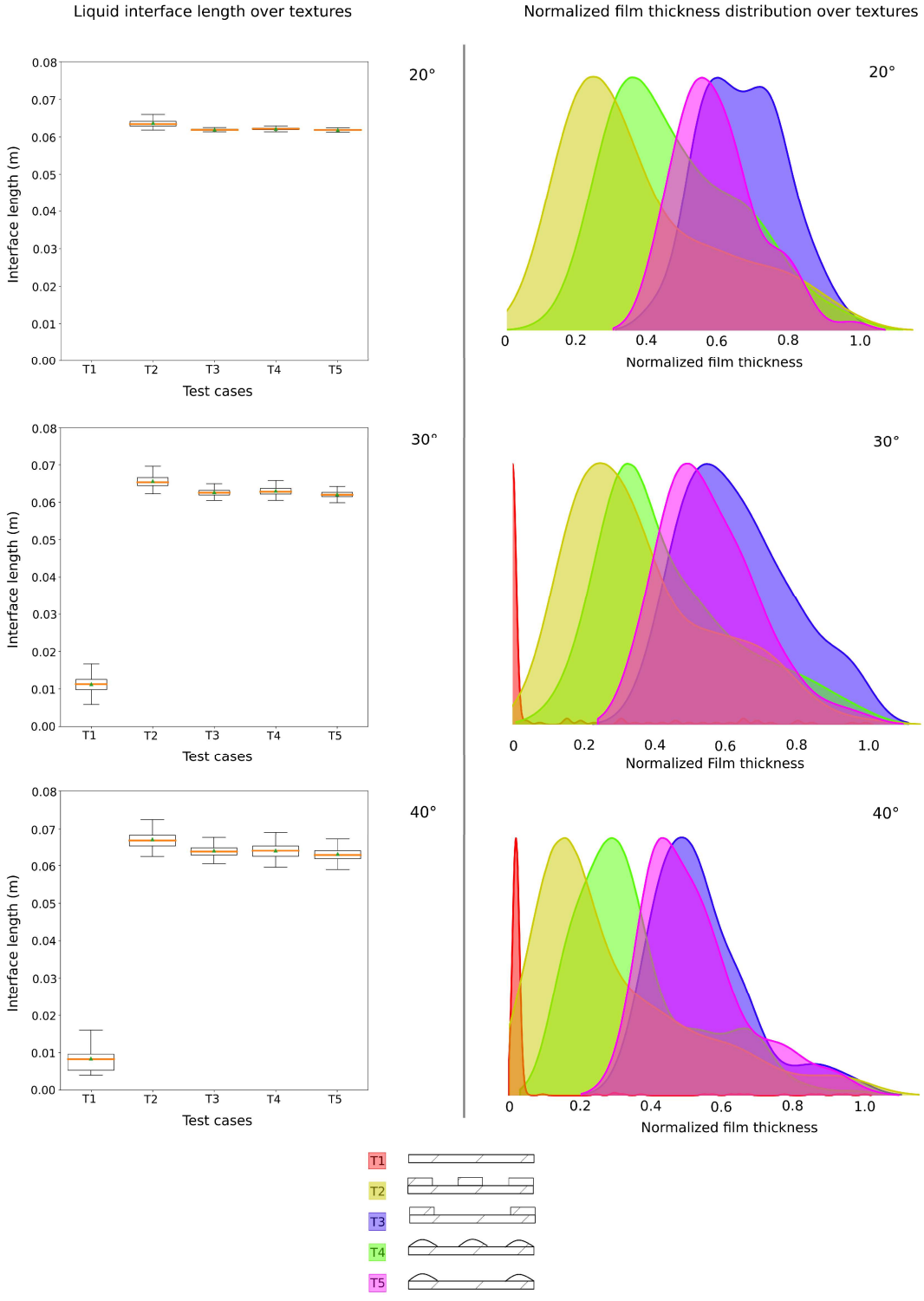

Fig. 4. Effect of textures on the interfacial length and film thickness distribution

In the post-processing step, the interfacial length is computed for each exported time step after $t > 4$ s.This 1D array is then analyzed to compute the statistics of the interfacial area for each case. The left column of Figure 4 shows the Box-Whisker plots of these arrays. The right column displays the probability density functions (PDF) of the film thickness virtually measured at 7 cm downstream of the inlet at $t > 4$ s. The box plots illustrate that in cases with no textures ($T1$), the interfacial length decreases with increasing contact angles. This finding is consistent with the results from the previous plots, which showed highly partially wetted surfaces at higher contact angles. With the introduction of textures, however, there is a notable increase in the mean length of the gas-liquid interface. The mean interfacial length increases by a factor of six in cases with contact angles of 30 and 40 when surface textures are introduced. Interestingly, the trend in the mean values is the same across all contact angles, with texture $T2$ consistently having the highest mean interfacial length value, followed by texture $T4$. This finding agrees with the results obtained in the previous section, where we predicted that textures $T2$ and $T4$ enable more high-frequency waves on top of the low-frequency waves, compared to the textures $T3$ and $T5$. In all cases, the obtained mean values are greater than the length of the domain itself, suggesting that the textures introduce wrinkles in the film interface, leading to a larger contact area and hence higher absorption potential.
The PDF plots reveal that film thickness values remain nearly constant in the absence of textures, indicating an absence of a wavy interface. Moreover, the plots indicate that in the case of highly dense textures ($T2$ and $T4$), film thickness values are widely dispersed, with high and low-amplitude waves resulting in more crests and troughs and hence a higher interfacial area. Conversely, textures $T3$ and $T5$ exhibit more uniform distribution, mainly with low amplitude waves, leading to a slightly smoother surface. Additionally, the distribution plot suggests that rectangular-shaped structures have a wider range of film thickness values than semi-circular structures. Nonetheless, the textured wall has improved the interfacial film length and eliminated partial wetting in all cases ($T2, T3, T4, T5$), regardless of the shape and frequency of the structures.

C. Experimental observations and outlook

The numerical results suggest that the presence and density of textures strongly influence variations in film thickness. Furthermore, texturing can alleviate the partial wetting observed at low Reynolds numbers. The accompanying experimental campaign confirmed that partial wetting occurs below Re 300, where the wetted area fraction can be less than 0.25 for Re below 100 (see Figure 5). Upon introducing textures, the wetted area fractions increased in all textured cases. During the dewetting tests, textured surfaces were able to maintain more than 80% wetting even at Re around 50, as predicted by the simulations. Importantly, repeated experiments showed that increasing texture density could significantly enhance film waviness, reaching a maximum point beyond which it acts like a flat surface. In future work, point-wise measurements will be used to quantitatively assess the SPH predictions for waviness and compile detailed measurements as a reference solution for SPH modeling studies.

VI. Conclusion

1) The hydrodynamics and statistics of a quasi-steady state liquid film have been analyzed in a falling film reactor with and without a textured wall.
2) Studies reveal that introducing textures on the walls alleviates partial wetting and spreads the liquid on the wall surface. It also enhances the gas-liquid interfacial area by forming wavy structures.
3) The introduction of textures also increases the gas-liquid interface length by six-folds, which significantly affects the interfacial area.

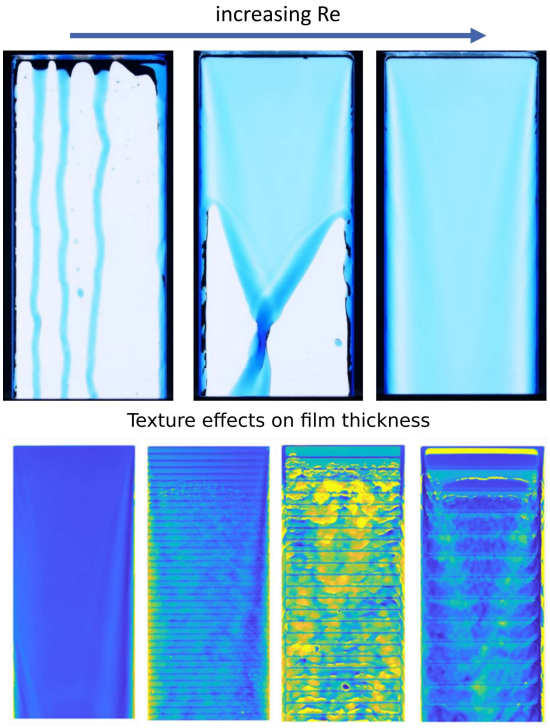

Fig. 5. Top: Effect of Re on partial wetting on smooth surfaces. Bottom: Developing waves with textured surfaces. The colour map indicates film thickness.

Acknowledgment

This work was performed on the HoreKa supercomputer funded by the Ministry of Science, Research and the Arts Baden-Württemberg and by the Federal Ministry of Education and Research. The study is financially supported by the Friedrich and Elisabeth Boysen Foundation.

References

[1] D. W. Green and R. H. Perry, *Perry's Chemical Engineers' Handbook, Eighth Edition*, 8th ed. New York: McGraw-Hill Education, 2008.

[2] P. N. Yoshimura, T. Nosoko, and T. Nagata, "Enhancement of mass transfer into a falling laminar liquid film by two-dimensional surface waves-some experimental observations and modeling," *Chemical Engineering Science*, vol. 51, no. 8, pp. 1231–1240, 1996.

[3] J. Hu, X. Yang, J. Yu, and G. Dai, "Numerical simulation of carbon dioxide (CO2) absorption and interfacial mass transfer across vertically wavy falling film," *Chemical Engineering Science*, vol. 116, pp. 243–253, 2014. [Online]. Available: http://dx.doi.org/10.1016/j.ces.2014.05.002

[4] L. K. Doraiswamy and D. Uner, *Chemical reaction engineering : beyond the fundamentals*, 1st ed. New York: Taylor '&' Francis, 2014.

[5] K. R. Putta, F. A. Tobiesen, H. F. Svendsen, and H. K. Knuutila, "Applicability of enhancement factor models for CO2 absorption into aqueous MEA solutions," *Applied Energy*, vol. 206, no. February, pp. 765–783, 2017. [Online]. Available: https://doi.org/10.1016/j.apenergy.2017.08.173

[6] G. Zahedi, A. Jahanmiri, A. Elkamel, and A. Lohi, "Mathematical modeling, simulation, and experimental verification of CO2 removal in a turbulent contact absorber," *Chemical Engineering and Technology*, vol. 29, no. 8, pp. 916–922, 2006.

[7] S. Norouzbahari, S. Shahhosseini, and A. Ghaemi, "CO2 chemical absorption into aqueous solutions of piperazine: Modeling of kinetics and mass transfer rate," *Journal of Natural Gas Science and Engineering*, vol. 26, pp. 1059–1067, 2015. [Online]. Available: http://dx.doi.org/10.1016/j.jngse.2015.07.048

[8] P. Bandi, M. Modigell, S. Groß, A. Reusken, L. Zhang, Y. Heng, W. Marquardt, and A. Mhamdi, "On reduced modeling of mass transport in wavy falling films," *AIChE Journal*, vol. 64, no. 6, pp. 2265–2276, 2018.

[9] H. Li, F. Yi, X. Li, A. N. Pavlenko, and X. Gao, "Numerical Simulation for Falling Film Flow Characteristics of Refrigerant on the Smooth and Structured Surfaces," *Journal of Engineering Thermophysics*, vol. 27, no. 1, pp. 1–19, 2018.

[10] R. K. Singh, J. Bao, C. Wang, Y. Fu, and Z. Xu, "Hydrodynamics of countercurrent flows in a structured packed column: Effects of initial wetting and dynamic contact angle," *Chemical Engineering Journal*, vol. 398, p. 125548, 2020. [Online]. Available: https://doi.org/10.1016/j.cej.2020.125548

[11] Y. Haroun, D. Legendre, and L. Raynal, "Volume of fluid method for interfacial reactive mass transfer: Application to stable liquid film," *Chemical Engineering Science*, vol. 65, no. 10, pp. 2896–2909, 2010. [Online]. Available: http://dx.doi.org/10.1016/j.ces.2010.01.012

[12] L. Yang, E. A. Peters, L. Fries, Y. M. Harshe, J. A. Kuipers, and M. W. Baltussen, "Direct numerical simulation of mass transfer and mixing in complex two-phase systems using a coupled volume of fluid and immersed boundary method," *Chemical Engineering Science: X*, vol. 5, p. 100059, 2020. [Online]. Available: https://doi.org/10.1016/j.cesx.2020.100059

[13] M. R. Davidson and M. Rudman, "Volume-of-Fluid Calculation of Heat or Mass Transfer across Deforming Interfaces in Two-Fluid Flow," *Numerical Heat Transfer, Part B: Fundamentals*, vol. 41, no. 3-4, pp. 291–308, 2002. [Online]. Available: https://doi.org/10.1080/104077902753541023

[14] A. A. Onea, "Numerical simulation of mass transfer with and without first order chemical reaction in two-fluid flows," Ph.D. dissertation, Universität Karlsruhe. Fakultät für Maschinenbau (MACH), 2012. [Online]. Available: DOI: 10.5445/IR/1000005765

[15] C. Yang and Z. S. Mao, "Numerical simulation of interphase mass transfer with the level set approach," *Chemical Engineering Science*, vol. 60, no. 10, pp. 2643–2660, 2005.

[16] D. Bothe and S. Fleckenstein, "A Volume-of-Fluid-based method for mass transfer processes at fluid particles," *Chemical Engineering Science*, vol. 101, pp. 283–302, 2013. [Online]. Available: http://dx.doi.org/10.1016/j.ces.2013.05.029

[17] L. E. N. Bird R. Byron, Stewart Warren E., *Transport Phenomena*, 2nd ed. Wiley, 2006.

[18] D. Darmana, N. G. Deen, and J. A. Kuipers, "Detailed 3D modeling of mass transfer processes in two-phase flows with dynamic interfaces," *Chemical Engineering and Technology*, vol. 29, no. 9, pp. 1027–1033, 2006.

[19] J. G. Khinast, A. A. Koynov, and T. M. Leib, "Reactive mass transfer at gas-liquid interfaces: Impact of micro-scale fluid dynamics on yield and selectivity of liquid-phase cyclohexane oxidation," *Chemical Engineering Science*, vol. 58, no. 17, pp. 3961–3971, 2003.

[20] K. B. Deshpande and W. B. Zimmerman, "Simulations of mass transfer limited reaction in a moving droplet to study transport limited characteristics," *Chemical Engineering Science*, vol. 61, no. 19, pp. 6424–6441, 2006.

[21] S. Radl, A. Koynov, G. Tryggvason, and J. G. Khinast, "DNS-based prediction of the selectivity of fast multiphase reactions: Hydrogenation of nitroarenes," *Chemical Engineering Science*, vol. 63, no. 12, pp. 3279–3291, 2008.

[22] D. Gründing, S. Fleckenstein, and D. Bothe, "A subgrid-scale model for reactive concentration boundary layers for 3D mass transfer simulations with deformable fluid interfaces," *International Journal of Heat and Mass Transfer*, vol. 101, pp. 476–487, 2016.

[23] G. Y. Soh, G. H. Yeoh, and V. Timchenko, "A CFD model for the coupling of multiphase, multicomponent and mass transfer physics for micro-scale simulations," *International Journal of Heat and Mass Transfer*, vol. 113, pp. 922–934, 2017. [Online]. Available: http://dx.doi.org/10.1016/j.ijheatmasstransfer.2017.06.001

[24] J. Maes and C. Soulaine, "A unified single-field Volume-of-Fluid-based formulation for multi-component interfacial transfer with local volume changes," *Journal of Computational Physics*, vol. 402, p. 109024, 2020. [Online]. Available: https://doi.org/10.1016/j.jcp.2019.109024

[25] D. Sebastia-Saez, S. Gu, P. Ranganathan, and K. Papadikis, "3D modeling of hydrodynamics and physical mass transfer characteristics of liquid film flows in structured packing elements," *International Journal of Greenhouse Gas Control*, vol. 19, pp. 492–502, 2013. [Online]. Available: http://dx.doi.org/10.1016/j.ijggc.2013.10.013

[26] D. Sebastia-Saez, S. Gu, and P. Ranganathan, "Volume of fluid modeling of the reactive mass transfer of CO2 into aqueous amine solutions in structured packed elements at microscale," *Energy Procedia*, vol. 63, no. 0, pp. 1229–1242, 2014.

[27] J. Hu, X. Yang, J. Yu, and G. Dai, "Carbon dioxide (CO2) absorption and interfacial mass transfer across vertically confined free liquid film-a numerical investigation," *Chemical Engineering and Processing: Process Intensification*, vol. 111, pp. 46–56, 2017. [Online]. Available: http://dx.doi.org/10.1016/j.cep.2016.11.002

[28] J. K. Min and I. S. Park, "Numerical study for laminar wavy motions of liquid film flow on vertical wall," *International Journal of Heat and Mass Transfer*, vol. 54, no. 15-16, pp. 3256–3266, 2011. [Online]. Available: http://dx.doi.org/10.1016/j.ijheatmasstransfer.2011.04.005

[29] P. Español and M. Revenga, "Smoothed dissipative particle dynamics," *Phys. Rev. E*, vol. 67, p. 026705, Feb 2003.

[30] X. Y. Hu and N. A. Adams, "Angular-momentum conservative smoothed particle dynamics for incompressible viscous flows," *Physics of Fluids*, vol. 18, no. 10, p. 101702, 2006.

[31] S. Adami, X. Y. Hu, and N. A. Adams, "A new surface-tension formulation for multi-phase {SPH} using a reproducing divergence approximation," *Journal of Computational Physics*, vol. 229, no. 13, pp. 5011 – 5021, 2010.

[32] M. B. Liu and G. R. Liu, "Smoothed particle hydrodynamics (sph): an overview and recent developments," *Archives of Computational Methods in Engineering*, vol. 17, no. 1, pp. 25–76, 2010.

[33] A. Hoffmann, I. Ausner, J. U. Repke, and G. Wozny, "Fluid dynamics in multiphase distillation processes in packed towers," *Computers & Chemical Engineering*, vol. 29, no. 5, pp. 1433–1437, 2005.

[34] A. Hoffmann, I. Ausner, J.-U. Repke, and G. Wozny, "Detailed investigation of multiphase (gas–liquid and gas–liquid–liquid) flow behaviour on inclined plates," *Chemical Engineering Research and Design*, vol. 84, no. 2, pp. 147–154, 2006.